Fluid bilayer structure determination by the combined use of x-ray and neutron diffraction

I. Fluid bilayer models and the limits of resolution

Michael C. Wiener and Stephen H. White
Department of Physiology and Biophysics, University of California, Irvine, California 92717 USA

ABSTRACT This is the first in a series of papers concerned with methods for the determination of the structures of fluid phospholipid bilayers in the liquid-crystalline (L_α) phase. The basic approach is the joint refinement of quasimolecular models (King and White, 1986. *Biophys. J.* 49:1047–1054) using x-ray and neutron diffraction data. We present here (*a*) the rationale for quasimolecular models, (*b*) the nature of the resolution problem for thermally disordered bilayers, and (c) an analysis of the resolution of experiments in which Gaussian functions are used to describe the distribution of submolecular components. We show that multilamellar liquid-crystalline bilayers are best described by the convolution of a perfect lattice function with a thermally disordered bilayer unit cell. Lamellar diffraction measurements on such a system generally yield only 5–10 orders of diffraction data from which transbilayer profiles of the unit cell can be constructed. The canonical resolution of these transbilayer profiles, defined as the Bragg spacing divided by the index of the highest recorded diffraction order, is typically 5–10 Å. Using simple model calculations, we show that the canonical resolution is a measure of the widths of the distributions of constituents of the unit cell rather than a measure of the spatial separation of the distributions. The widths provide a measure of the thermal motion of the bilayer constituents which can be described by Gaussian functions. The equilibrium positions of the centers of the distributions can be determined with a precision of 0.1–0.5 Å based upon typical experimental errors.

INTRODUCTION

The lipid bilayers of natural membranes generally exist in a fluid state which occurs above the gel to liquid-crystalline phase transition temperature (see review by Bretscher and Raff, 1975). Knowledge of the structure of such bilayers is important for understanding fundamental biological processes mediated by or occurring within membranes. X-Ray and neutron diffraction have played a central role in understanding bilayer structure and have been particularly useful for studying multilamellar arrays of bilayers (see review by Franks and Levine, 1981). Unfortunately, the high degree of thermal disorder of fluid bilayers has made the interpretation of their structures difficult. Indeed, even the use of the term "structure" is problematic in these systems and must be clarified. We have therefore undertaken an extensive investigation of methods for extracting the maximum amount of useful structural information from membrane diffraction experiments. We have found that neutron and x-ray diffraction measurements can be combined through joint-refinement procedures to arrive at a surprisingly detailed image of the transbilayer distribution of the principal structural groups of the phospholipids comprising the bilayer. This is the first of a series of papers describing the results of our efforts.

We are accustomed to viewing highly detailed images of protein crystallographic structures in which the mean relative positions of small groups of atoms are well-defined and measurable. Diffraction studies of phospholipid crystals at low hydrations can provide a similar view of phospholipid molecules (see review by Hauser et al., 1981). Thermal motion and disorder preclude such images for fluid bilayers. However, it is reasonable to consider the average transbilayer distribution of multiatom submolecular groups comprising the lipids and proteins (King and White, 1986; Jacobs and White, 1989). The "image" of the membrane in this case consists of the average spatial distribution of the submolecular groups projected onto a line normal to the plane of the membrane from which the relative intergroup distances can be determined. It is this image which we take as "the structure" of the fluid bilayer. Even though it does not provide direct information about membrane structure in the other two dimensions (bilayer plane), this one-dimensional image is crucial for understanding how lipid composition and proteins affect the transbilayer distributions of submolecular groups.

A multilamellar lattice of thermally disordered bilayer unit cells typically yields 5–10 orders of diffraction data from which a transbilayer profile with a canonical resolution of 5–10 Å can be constructed (Levine and Wilkins, 1971; Franks and Levine, 1981; Blaurock, 1982). These profiles have provided a variety of structural information, such as the interbilayer headgroup

Address correspondence to Dr. White.

0006-3495/91/01/162/12 $2.00

separation (e.g., Levine and Wilkins, 1971) and the presence of transbilayer acyl chain interdigitation (e.g., McIntosh et al., 1983). The resolution of bilayer diffraction experiments can be functionally increased using neutron diffraction by taking advantage of the difference in neutron scattering length of hydrogen and deuterium (Blasie et al., 1975; Schoenborn, 1975; Worcester, 1975). Specific labeling with deuterium at various positions within a lipid molecule makes it possible to locate the transbilayer position and distribution of the label with a precision of better than 1 Å (Worcester and Franks, 1976; Büldt et al., 1979; Zaccai et al., 1979). Such labeling has proven especially useful for determining the transbilayer location of added solute molecules such as hexane (White et al., 1981) and peptides (Jacobs and White, 1989).

The general difficulty with specific labeling experiments is the amount of chemical and diffraction work which must be done. For each labeled position, such as the acyl chain C(2) carbon of a phospholipid (King and White, 1986), one must typically repeat the diffraction experiment six times because the protonated and deuterated samples must be examined at several mole fractions of D_2O in the aqueous phase to scale different data sets to one another, to reduce experimental uncertainty, and to determine the phasing. Heroic efforts are required to label enough different positions of the lipid molecule to arrive at a detailed image of the bilayer (Büldt et al., 1979; Zaccai et al., 1979). The quasimolecular modeling approach of King and White (1986) can reduce considerably the amount of neutron data required to arrive at a useful description of the transbilayer distribution of the constituents of the lipid molecule. This approach involves the representation of the fluid phospholipid molecule as a sum of Gaussian functions representing the positions and distributions of submolecular components such as the double bonds, carbonyl groups, and phosphocholine headgroup.

We will describe in this and subsequent papers of the series the extension of the quasimolecular modeling method to include both neutron and x-ray diffraction data and will demonstrate the usefulness of combining the two diffraction methods for the joint refinement of bilayer profiles. Before one can appreciate and have confidence in jointly refined quasimolecular models, one must first fully explore the meaning and limits of resolution in the context of the fluid bilayer. That is the purpose of this paper. We describe in turn (*a*) the rationale for quasimolecular models, (*b*) the nature of the resolution problem for fluid bilayers, and (*c*) an analysis of the spatial resolution of experiments in which Gaussian functions are used to describe the distribution of submolecular components.

QUASIMOLECULAR MODELING: MULTI-GAUSSIAN REPRESENTATIONS OF BILAYERS

The principal objective of molecular modeling in bilayer diffraction studies should be to construct a real-space model for the distribution of matter across the bilayer which is both realistic and quantitatively useful. All modeling procedures involve the construction of a real-space model representing the transbilayer distribution of scattering length or electron density whose Fourier transformation will yield accurate estimates of observed structure factors in reciprocal space. A lipid bilayer can be equally well represented in reciprocal space by many different real-space models including strip models (Worthington, 1969; King and White, 1986), "smoothed" strip models (Franks et al., 1982), "disordered" crystalline models (Hitchcock et al., 1975; Franks, 1976; Worcester and Franks, 1976; Dorset et al., 1987), Gaussian models (Rand and Luzzati, 1968; Mitsui, 1978; Büldt et al., 1979; King and White, 1986), and hybrid Gaussian/strip models (Wiener et al., 1989). However, the various models are not equally useful in real space. The disadvantage of strip models is that the boundaries between different regions of the bilayer are discontinuous and thus unrealistic for a liquid-crystalline phase. This can be circumvented by appropriate smoothing with a Debye-Waller factor (Franks and Levine, 1981; Franks et al., 1982) but one then encounters the problem of determining appropriate and meaningful Debye-Waller factors for the strips. More important, the compositions of the strips are generally unknown. The "disordered" crystalline model suffers from the fact that one must have the crystalline coordinates and, as with smoothed strip models, accurate knowledge of how to implement the disordering by means of Debye-Waller factors. Such knowledge is equivalent to knowing the molecular details of the transition from the crystalline to fluid state.

The Gaussian quasimolecular model is a logical extension of the disordered crystal model in that Debye-Waller factors for small crystals are rigorously derived by considering the Gaussian-distributed deviations of atoms from their equilibrium positions (Warren, 1969). The one-dimensional projection of a perfect crystalline lipid structure along the bilayer normal is a series of sharp, approximately δ-function, peaks. Thermal disorder, represented by the Debye-Waller factors of the constituent atoms, will broaden these peaks, leading to the "disordered" crystalline model. As thermal disorder increases, the broadened adjacent atomic peaks overlap making it impossible to resolve them individually. It is logical to merge these overlapping and unresolvable atomic distributions into a single Gaussian function

representing an appropriate multiatomic grouping. The quasimolecular model thus appropriately consists of a series of such Gaussians which account for all of the atomic mass of the unit cell. The positions of the Gaussians represent the time-averaged positions of the submolecular pieces whereas their widths describe the range of thermal motion of the pieces (Willis and Pryor, 1975). Because the quasimolecular model accounts for thermal motion from the start, Debye-Waller terms are not included in the transform. The use of Gaussian distributions implies that the motions of these multiatomic distributions are primarily harmonic. In crystal structures, some atoms probably undergo anharmonic motion; however, molecular dynamics calculations (Kuriyan et al., 1986) suggest that these regions are best described by a series of Gaussians rather than a single non-Gaussian distribution.

STRUCTURAL DISORDER AND RESOLUTION

In membrane diffraction experiments, the Fourier transbilayer density profiles obtained from the phased structure factors are assigned a *canonical resolution* of d/h_{max}, where d is the one-dimensional Bragg spacing and h_{max} is the highest order of diffraction observed. This definition of resolution, obtained directly from Bragg's Law, is commonly used in macromolecular crystallography (Glusker, 1981). The resolution of diffraction experiments has also been estimated from a consideration of diffraction as an optical imaging problem using Rayleigh's criterion for Fraunhofer diffraction by an aperture. For a circular or single-slit aperture, the canonical d/h_{max} resolution is scaled by 0.61 and 0.5, respectively (Bragg and West, 1930); both of these resolution values have been quoted (e.g., Perutz, 1942; Franks and Levine, 1981). When we refer to "resolution" in this and subsequent papers, we will mean the unscaled canonical definition.

With a canonical resolution of 5–10 Å, the structural information obtainable from lamellar membrane diffraction appears rather limited. However, in seeming contradiction to this resolution, certain features of the bilayer that are principal scattering centers can be resolved and their positions accurately determined. For instance, the high electron density peaks in the bilayer profiles obtained from x-ray diffraction are assigned to the phosphate moieties and the distance between them ($d_{p\text{-}p}$) is frequently cited to a precision of 1 Å or better (Ranck et al., 1977; Inoko and Mitsui, 1978; Janiak et al., 1979; McIntosh and Simon, 1986). McIntosh and Simon (1986) demonstrated with model calculations that a shift of several angstrom in the phosphate position within the bilayer would result in observable changes in both the real-space Fourier density profile and the reciprocal-space continuous transform. Wiener et al. (1989) compared the locations of the phosphate peak in Fourier profiles of diffraction data to those of the hybrid Gaussian/strip and strip models used to fit the data and found the discrepancy in positions between a model and its Fourier reconstruction to be <4 Å. In utilizing one-dimensional models to interpret bilayer diffraction data, parameters of the model are often determined with a precision of 1 Å or better (Rand and Luzzati, 1968; King and White, 1986; Wiener et al., 1989; White and Jacobs, 1989). The conflict between the canonical and apparent resolution can be resolved by a careful consideration of the nature of the disorder found in multilamellar fluid bilayer systems.

The resolution of a diffraction experiment can be limited by the amount of data collected or by the disorder of the unit cell and/or the crystalline lattice. A well-ordered lamellarlike phospholipid crystal with a Bragg spacing of $d \approx 50$ Å whose atoms are confined to positions on the order of an atomic diameter (≈ 2 Å) should produce ~ 25 ($=h_{max} = 50$ Å/2 Å) orders of diffracted intensity as observed by Sakurai et al. (1977) and Suwalsky and Duk (1987). The molecules of the unit cell in this case constitute what we shall call a *high-resolution structure* and the Fourier transformation using all of the observable structure factors yields a *fully resolved image* of the unit cell. If one collected only a small number of orders of data, the resulting image would be a *partially resolved image* of the high-resolution structure. In contrast, a fluid bilayer structure is inherently a *low-resolution structure* because thermal motion causes the atoms of the molecules to be broadly distributed over distances of 5–10 Å. One can expect to observe no more than 5–10 diffraction orders in this case regardless of the carefulness of the sample preparation, the sensitivity of the detector, or the intensity of the source. The Fourier transformation using all of the structure factors thus yields a fully resolved image of the low-resolution structure.

The difference in the number of diffraction orders observed from crystalline and liquid-crystalline phases is a direct consequence of the spatial distribution of matter resolvable over the time-course of a diffraction experiment. Individual atoms or small groups of atoms are discernible in the high-resolution structure of a crystal whereas the thermal disorder of the liquid-crystal causes these distributions to overlap, producing a low-resolution structure. The physically appropriate structural subunits of the liquid-crystal are these overlapping multiatomic "quasimolecular" pieces. For both crystalline and liquid-crystalline materials, the intensities of the diffracted x-rays can be accurately measured and in

both cases models of appropriate resolution can be constructed which allow one to refine the structural image with great sensitivity. We show in this paper that the average positions and widths of the distributions of multiatomic molecular "fragments" comprising the fluid bilayer system can be determined with considerable precision. This means that it is not correct to assume that the low canonical resolution of the bilayer diffraction experiment makes it impossible to determine distances and distributions to better than d/h_{max}. On the contrary, if thermal motion is the only cause of disorder, then one can construct very accurate fully resolved images of the low-resolution structure.

One normally distinguishes three types of disorder in diffraction experiments (Hosemann and Bagchi, 1962; Schwartz et al., 1975; Blaurock, 1982). Disorder of the first kind is thermal disorder in which the atoms or molecular fragments oscillate about well-defined positions within the unit cell. A sample with only this type of disorder will have a unit cell of well-defined composition and a lattice with a high degree of long-range order. Thus, even though the molecules of the unit cell are vibrating, the mean positions are well-defined and identical for all equivalent lattice positions. Disorder of the second kind applies to the situation where long-range order and/or uniform unit-cell composition are lacking. For example, a pellet of biological membranes can consist of stacks of membranes of constant composition but with variable water spacing between membranes so that over long distances there is a loss of spatial coherence (i.e., a decrease in correlation length) between equivalent intrabilayer positions for pairs of membranes separated by many intervening membranes. A third type of disorder is orientational disorder which is related solely to the macroscopic features of a particular sample. For example, a single crystal of salt will produce discrete diffraction spots at well-defined angular positions relative to the x-ray beam. If the crystal is broken up to form a powder, the numerous small crystallites will be oriented at various angles with respect to one another and the x-ray beam so that ringlike diffraction spots are produced. The diffracting lattices can be nearly perfect in both cases.

Thermal disorder can be easily distinguished experimentally from other types of disorder. Consider a lamellar sample with perfect lattice in a well-focused x-ray beam incident along the x-axis. Orient the sample so that the bilayer normal is parallel to the positive z-axis. As the normal is rotated through an angle 2Θ about an axis parallel to the y-axis, the lamellar diffracted intensities satisfying the Bragg condition $2d \sin \Theta = h \lambda$ will be observed along the z-axis (meridian) at angular positions $\approx 2h\Theta$. The diffraction spots observed represent the convolution of the beam profile with the Bragg peaks and will be perfect images of the x-ray beam if the lattice is perfect (ignoring domain-size effects). However, the shape of the images will differ from the incident beam if the sample or its lattice is disordered. For example, a sample with orientational disorder resulting from the macroscopic fragmentation will consist of a mosaic of pieces disoriented with respect to one another by a range of angles ϕ. A sample with this type of disorder will have diffraction spots spread into arcs of angular length ϕ on the yz-plane centered on the x-axis. If the pieces of the mosaic are each perfect crystals, the widths of the spots in the z direction will be the same as the beam and constant for all h (assuming a perfectly focused beam). An example of this situation is shown in Fig. 1 *A* for a neutron diffraction study of oriented lipid multilayers containing a hydrophobic peptide (Jacobs and White, 1989). The widths of the peaks measured along the z-axis (Fig. 1 *B*) are identical to the width of the incident beam (data not shown). If the lattice itself had been disordered due to irregular bilayer spacing or to nonuniform unit-cell composition, these widths would have progressively increased with h (Blaurock, 1982). In the analysis of line widths, it is crucial that the effects of finite domain size and beam focusing be taken into account (see Franks and Lieb [1979] and Schoenborn [1983]).

In a series of elegant experiments utilizing synchrotron radiation and very high-resolution monochromators, Smith et al. (1987) demonstrated that arrays of L_α phosphatidylcholine bilayers form virtually perfect one-dimensional lattices and that the widths of the observed Bragg peaks arise only from finite domain size. Most of their experiments were performed on highly oriented films at various hydration levels. This high degree of orientation, imperative for their detailed investigations of Bragg peak line-shape (Smith et al., 1987) and bilayer in-plane structure (Smith et al., 1988; Sirota et al., 1988), is not required for formation of highly ordered lattices. The observed line-widths of Bragg peaks of oriented DMPC-cholesterol bilayers, prepared in a similar fashion to our samples, can be satisfactorily explained on the basis of purely instrumental effects (Franks and Lieb, 1979). Specifically, the convolution of a Gaussian beam profile with an aperture representing the sample length in the beam adequately fit the measured line-widths. The result of the application of Franks and Lieb's (1979) analysis to the diffraction data for L_α DOPC multilayers used in subsequent papers of this series is shown in Fig. 2. Examples of the densitometer traces of the x-ray films are shown in Fig. 2 *A*. The line-width analysis shown in Fig. 2 *B* demonstrates that there is no line-width broadening other than that expected for finite domain size and beam-focus effects. Thus, the samples used in the work to be described in subsequent papers show only disorder

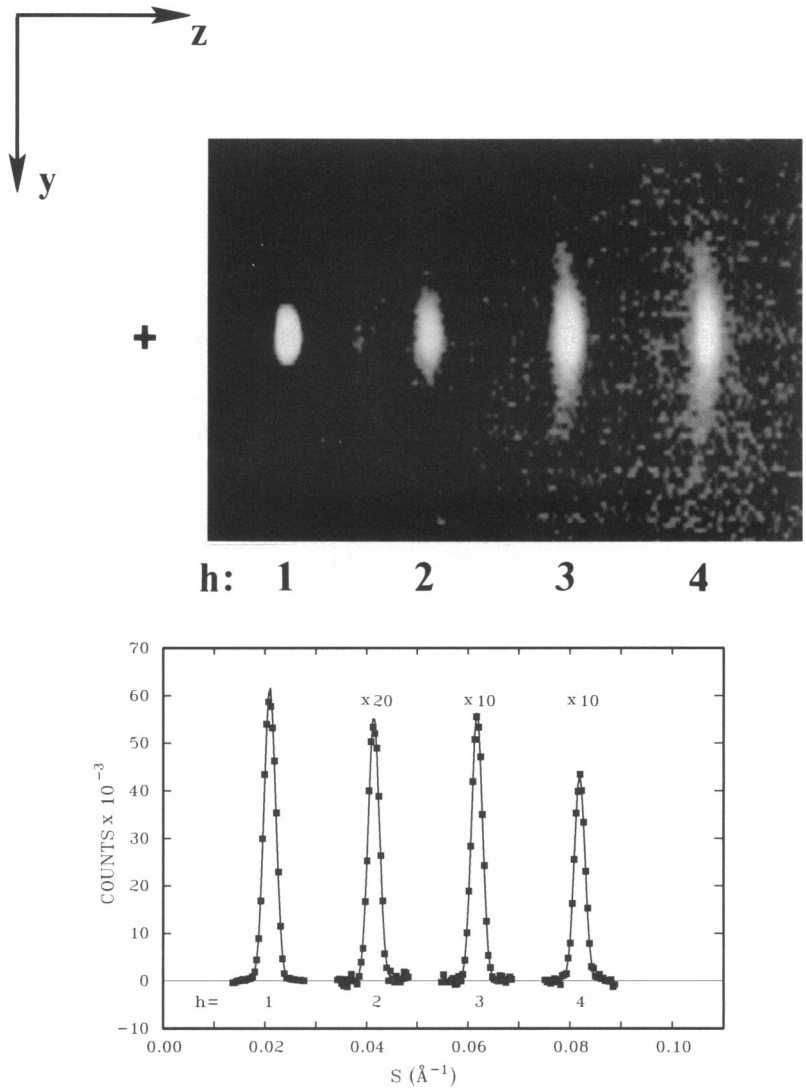

FIGURE 1 Neutron diffraction data from oriented DOPC multilayers containing the hydrophobic peptide Ala-Trp-Ala-*O-tert*-butyl (0.10 per lipid). The experiments from which these data are taken are described in Jacobs and White (1989). In this particular case, the Trp residue is specifically deuterated (five deuteriums) and the aqueous phase contains 10 mol% D_2O; 66% *RH* and $T = 23°C$. Similar results are obtained for peptide-free bilayers. The data were collected by standard ω scans using 0.1° increments from 0° to 6.5°. Using the conventions described in the text, ω represents angular rotations around the *y*-axis. A two-dimensional detector records the diffracted intensities in the *zy*-plane so that the diffraction peaks are distributed along the *z*-axis. A detector array is recorded for each value of ω. The + symbol shows the position of the incident beam. (*A*) Summed intensities obtained by summing together all of the ω arrays; the summed array is equivalent to the image one would obtain on a film in an x-ray diffraction experiment. Note the "smearing" around the *z*-axis due to the mosaic spread (disorientational disorder). (*B*) The background-corrected intensities of the diffracted peaks obtained from the summed arrays in *A* by scanning along the *z*-axis. Solid points are experimental measurements; lines are fitted Gaussian functions. The $h = 2$, 3, and 4 peaks have been multiplied by the factors shown. The 1/e half-widths ($\Delta S \approx 0.0015$ Å^{-1} or $\Delta\omega \approx 0.08°$) are independent of diffraction order and the same as the half-width of the incident beam. This means that the lattice disorder of the sample is very small.

of the first kind and a relatively small amount of disorientational disorder (mosaic spread $\phi \approx 10$–$20°$). This means the lattice is excellent with long-range order and uniform unit-cell composition so that the diffraction is limited only by thermal motion which reduces the intensity of higher order spots but does not affect their widths along the *z*-axis. With this type of disorder, one is completely justified in representing the unit-cell contents as a series of Gaussians whose widths describe the thermal motions of the represented pieces.

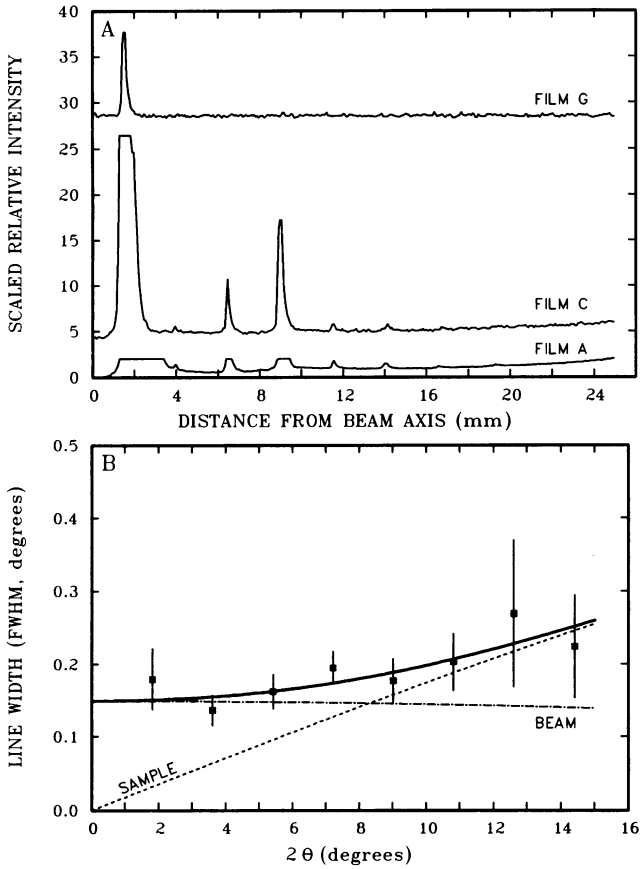

FIGURE 2 X-Ray difraction data from oriented DOPC multilayers at 66% *RH* and T = 23°C (no peptide). Ni-filtered CuK_α x-rays from a stationary anode microfocus generator (Spectro Equipment, Inc., North Royalton, OH) were focused with toroidal optics (Elliott, 1965) and the diffraction pattern was recorded on a stack of 10 DEF-5 films (Kodak Laboratory and Specialty Chemicals, Eastman Kodak Co., Rochester, NY). The films were scanned by a modified laser densitometer (model SLR-2D/1D; Zeineh [supplied by Biomed Instruments Inc.], Fullerton, CA). (*A*) Representative one-dimensional meridional densitometer scans of several films from a typical experiment. From bottom to top, scans of the first, third and seventh films are shown. Film A shows eight diffraction orders with the first, third and fourth orders saturating the film. Film C shows six orders; the first order is still truncated. Film G shows the first order. Scaling the density trace (with background fog subtracted out) of the Nth film by f^{N-1}, where f is the film factor, places all of the films in a stack on the same scale. Film C is scaled by f^2, where f = 3.2 for the film used (Phillips and Phillips, 1985) and offset along the ordinate for clarity. Note that films A and C are on the same relative scale, seen by examining peaks two, five and six, and that the noise scales with the signal in film C. Film G is scaled by 3.2^6 = 1073.7; however, in order to fit it into this plot, it has been reduced by a factor of 100. The observed first order intensity is roughly 50 times larger than the next largest fourth order and about 4,000 times larger than the smallest observed eighth order. The broadened first order in films A and C arises primarily from this large dynamic range between the first and other orders. The base of the first order may be four or five 1/e half-widths away from the peak position but this is still an appreciable intensity compared to the higher orders recorded on the film. Oriented multilayers for x-ray diffraction are formed on curved glass substrates which enable one to record all of the lamellar diffraction orders in a single experiment. The multilayers satisfying the Bragg condition for each order are at slightly different positions and the diffracted beam travels through varying lengths of the glass substrate. Integrated intensities can be corrected by the appropriate absorption factor for this geometry (Franks and Lieb, 1979). Just as different orders are at different positions on the glass substrate, the domain that gives rise to an observed diffraction order consists of bilayers at varying positions. The differential adsorption of these "microdomains," perhaps modulating thermal diffuse scatter, gives rise to the observed asymmetry of the line-shapes. The white radiation (bremsstrahlung) of the x-ray source may also contribute. As films farther down in the stack are scaled, much of this asymmetry becomes indistinguishable from background. (*B*) An analysis of diffraction line-broadening due to geometrical sample and beam effects using the approach of Franks and Lieb (1979). The full-width half-maxima of Bragg peaks are averages from three experiments and most of the peaks were obtained from several films in each experiment. Two factors contribute to the observed peak-width in this calculation. The projection of the beam from the Ewald sphere onto the flat film, approximated by a Gaussian function, is nearly constant with scattering angle 2θ, tailing off slightly with increasing angle. For a sample-to-film distance d_s, scattering angle 2θ and Gaussian beam of full-width half-maximum (FWHM) 2Δ, the FWHM of the projected beam is given by $2 \tan^{-1} [\Delta[\cos^2 (2\theta)]/d_s]$. The beam FWHM dominates at small angles. The other factor is from the finite length L of the sample in the beam; this box or aperture contributes a projected width proportional to sin 2θ. Specifically the FWHM arising from finite sample length is given by $2 \tan^{-1} [L[\cos (2\theta) \sin (2\theta)]/2d_s]$. The sample length FWHM dominates at larger angles. The convolution of these two terms gives rise to the observed line-widths. Optimal values of beam-width and sample length were determined from a nonlinear least-squares fit to this convolution, which can be expressed in terms of error functions (Hosemann and Bagchi, 1962, p. 64). For our data, a beam FWHM of 0.2 mm and a sample length of 1.4 mm, consistent with our experimental set-up, provided the best fit.

It might at first seem peculiar that stacks of fluid bilayers with a great deal of thermal disorder produce a one-dimensional lattice with excellent long-range order. Though the phase space trajectory of the unit cell is very complicated, each unit cell is subject to the same constraints and interactions so that the average transbilayer distribution of matter is precisely the same for each bilayer. Because the bilayer can be considered a quasiergodic system (Hosemann and Bagchi, 1962), this distribution of matter representing the time-averaged dynamical structure of a single bilayer is equivalent to the spatial ensemble average of many bilayers' configurations occurring at successive times which gives rise to the observed diffraction. Thus, if one selects a particular point z_i within a particular bilayer, the average scattering density at that point will be precisely the same as the average scattering density at a point n bilayers away located at $z_i + nd$. Fully resolved scattering density profiles of bilayers in a well-ordered lattice are therefore accurate representations of the average distribution of matter in the bilayers and can clearly reveal the thermal disorder which is an important feature of the fluid bilayer. The determination of thermal disorder provides information on the relative dynamics of different por-

tions of the molecule and is already a powerful technique in crystallography (Ringe and Petsko, 1986).

THEORY AND MODEL CALCULATIONS

We conclude from the above discussion that properly formed multilamellar fluid bilayers consist of a highly ordered lattice of thermally disordered unit cells, that the resolution is limited only by this unit-cell disorder, and that an appropriate representation of any multiatom submolecular group is as a Gaussian function. The distribution of scattering density within the unit cell is manifested by typical widths of submolecular groups that are wider than their corresponding hard-sphere diameters, indicative of the broadening of their distributions by thermal motion. However, the equilibrium positions of the centers of these scattering distributions are very well-defined and small deviations from these equilibrium positions are reflected in observably different structure factor amplitudes.

A very simple Gaussian model of the bilayer illustrates the effect of variation of structural parameters upon simulated diffraction data. Complete quasimolecular models (King and White, 1986) are considerably more complicated than this but the simpler Gaussian models described here give a reasonably accurate estimate of the resolution. The bilayer is centrosymmetric so that we can consider a "bilayer half" consisting of a single Gaussian distribution of unit area, with center Z_1, 1/e half-width A_1, and scattering amplitude b_1 whose scattering length density is given by

$$\rho(z) = [b_1/(A_1\sqrt{\pi})] \exp\{-[(z - Z_1)/A_1]^2\}. \quad (1)$$

For a bilayer of repeat d, with $z = 0$ defined as the bilayer center, the centrosymmetric unit cell consists of two Gaussians at $\pm Z_1$. For multilamellar arrays, the structure factors are sampled at discrete points in reciprocal space, $S = h/d$, where h is a nonnegative integer. These structure factors, denoted $F(h)$, are easily calculated from $\rho(z)$ (see King and White, 1986):

$$F(h) = 2b_1 \exp[-(\pi A_1 h/d)^2] \cdot \cos(2\pi Z_1 h/d). \quad (2)$$

The structure factor $F(h)$ (Eq. 2) is the product of three terms: the first term proportional to scattering amplitude b_1, an exponential containing the width A_1 of the distribution, and a cosine term containing its center Z_1. The exponential terms for two values of A_1 are shown in Fig. 3; these two values, 1 and 3 Å, are representative of the distributions of scattering material in crystals and liquid-crystals, respectively. The 3 Å value was chosen because it is typical of our earlier observations (King and White, 1986; Jacobs and White, 1989; Wiener et al., 1989) and this half-width corresponds to the 6 Å resolution expected for $h = 8$ and $d = 50$ Å. For x-ray diffraction (but not neutron diffraction), scattering length decreases slightly with increasing S (Warren, 1969; Bacon, 1975) as indicated for the 1 Å Gaussian by the dashed line calculated for a single methylene; this decrease is negligible for the 3 Å Gaussian. In the remainder of the paper, we ignore the dependence upon reciprocal space S of the x-ray scattering length.

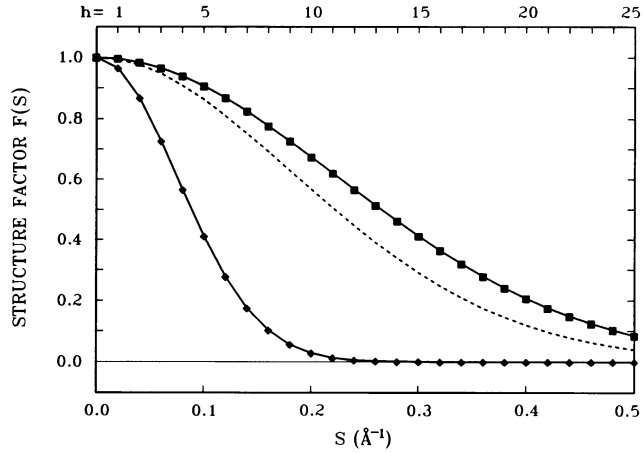

FIGURE 3 Structure factor amplitude from the exponential term of Eq. 2 as a function of reciprocal space S for several values of 1/e half-width A_1. For a bilayer of repeat $d = 50$ Å, the diffraction from lamellar arrays is observed at $S = 0.02$ h; the order h is indicated on the upper abscissa. The squares represent $A_1 = 1$ Å, a typical 1/e half-width for an atom in a crystal. The dotted line shows the slight decrease in amplitude arising from the decrease in x-ray scattering length with increasing S (Warren, 1969) and is calculated for a single CH_2 group. The diamonds represent $A_1 = 3$ Å, appropriate for liquid-crystals, with a negligible x-ray scattering length correction.

To compare the exponential terms (from Eq. 2) for the two 1/e half-widths within the context of an experiment, we define a threshold δF which is the amplitude of the smallest structure factor detectable. In our x-ray diffraction experiments on oriented L_α DOPC (to be described in a later paper), the ratio of smallest ($h = 2$) to largest ($h = 1$) structure factors is 0.035. A series of very long exposures, carried out to search for higher ($h > 8$) orders, reduced this threshold slightly to 0.033. For the analysis of Fig. 3, where the first order is virtually equal to one, this ratio of 0.033 is also the value of the threshold structure factor δF. The difference between the decays of the 1 and 3 Å curves with increasing S, shown in Fig. 3, is dramatic. The highest observable diffraction order h_{max} can be read from Fig. 3 or calculated from

$$h_{max} = \mathrm{INT}[(d/\pi A)\sqrt{(-\ln \delta F)}], \quad (3)$$

where INT[. . .] means the integer truncation of the expression within the brackets. A diffraction experiment with the threshold $\delta F = 0.033$ would thus record 29 orders for a feature of 1/e half-width 1 Å, but only 9 orders for a feature of width 3 Å. The role of the intrinsic disorder of the liquid-crystalline unit cell in determining the number of observable structure factors is immediately obvious. Conversely, the number of observable structure factors provides an estimate of the appropriate length scale with which to describe the distribution of matter within the bilayer. We emphasize observable because it is imperative to observe all the structure factors that the structure itself yields in order to establish the resolution limits of the unit cell and to assure that the bilayer profile image is fully resolved.

The structure factors $F(h)$ are the coefficients of the Fourier series representation of the bilayer. The nine order reconstructions of the two model distributions, centered at $z = Z_1$, are shown in Fig. 4. For the $A_1 = 3$ Å distribution, nine orders is the limit imposed by the structure; consequently, the distribution is well-approximated by the Fourier series and is free of termination/truncation artifacts. The ideal experiment records all (within δF) of the nonzero $F(h)$ so that the corresponding profile is a very accurate fully resolved representation. Conversely, for the $A_1 = 1$ Å (crystal) distribution, the nine-order profile does not provide an accurate representation. The center of the distribution is well-located but the width is too large and significant ripples

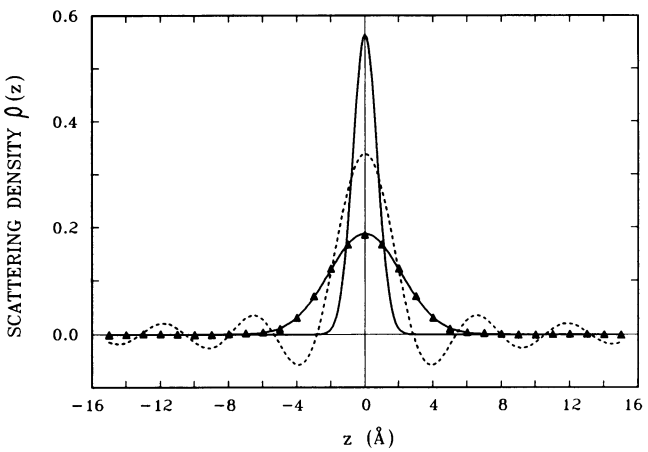

FIGURE 4 Model scattering length distributions and their corresponding nine order Fourier reconstructions. The nine order synthesis (*triangles*) of the $A_1 = 3$ Å distribution is a very good approximation to the actual Gaussian (*solid line*). Conversely, the nine order profile (*dashed line*) of the $A_1 = 1$ Å distribution has significant truncation error, seen as an exaggerated width of the central feature with ripples about the baseline. Excluding the higher order structure factors has a deleterious effect on the accuracy of the Fourier reconstruction of the narrower (1 Å) Gaussian.

are present. Clearly, an experiment measuring only nine orders from such a crystalline feature is far from ideal.

We now examine the ability of a typical diffraction experiment to resolve the structure of a bilayer consisting of several Gaussians. Consider the structure factors of a bilayer with two Gaussian distributions in each bilayer half. The center Z_2 of Gaussian 2, of 1/e half-width A_2 and scattering amplitude b_2, is displaced from Gaussian 1 by a distance ΔZ: $Z_2 = Z_1 + \Delta Z$. The structure factors of each Gaussian are described by an exponential envelope defined by the distribution width A_i, modulated by the cosine term involving the distribution center Z_i and scaled by b_i (Eq. 2). Nine orders of diffraction, observed in an experiment with the threshold $\delta F = 0.033$ for a Gaussian of width $A_1 = 3$ Å (*vide ut supra*), will be used in the subsequent calculations. If the calculated structure factors for the two Gaussians, centered at Z_1 and $Z_2 = Z_1 + \Delta Z$, are experimentally indistinguishable from the calculated structure factors of the two Gaussians, both centered at Z_1, then there is no "diffraction-based" justification for using two Gaussians separated by ΔZ to describe the bilayer. A single Gaussian of amplitude $b = b_1 + b_2$ will suffice. To compare these two models, two resolved Gaussians versus a single Gaussian feature, the crystallographic R factor is introduced, where the sum is over the observed structure factors:

$$R = \sum_h (\|F_1(h) + F_2(h; \Delta Z)| - |F_1(h) + F_2(h)\|) / \sum_h |F_1(h) + F_2(h)|. \quad (4)$$

The notation $F_2(h; \Delta Z)$ indicates that the Gaussian is centered at $Z_2 = Z_1 + \Delta Z$; otherwise the Gaussians are centered at Z_1. R is a convenient measure of the quality of the fit between model structure factors and observed data (King and White, 1986; Jacobs and White, 1989), or in the current discussion, a measure of the differences between two models. To place these calculated R factors in the relevant experimental context, the noise level of experimental data is described by a "self" R factor, R_s. A proper diffraction experiment yields a set of structure factors with corresponding experimental uncertainties: $F(h) \pm \sigma_h$. Summing the absolute values of σ_h and normalizing by the summed absolute values of $F(h)$ yields R_s:

$$R_s = \sum_h |\sigma_h| / \sum_h |F(h)|. \quad (5)$$

Values of $R > R_s$ indicate that an analysis of the observed $F(h)$ will be able to select the better of two distributions (two Gaussians versus a single Gaussian) used to model the data. If $R < R_s$, then the two distributions cannot be discriminated because their

structure factor differences are not discernible from the experimental noise level. R as a function of Z_1 and ΔZ is shown in Fig. 5 for two Gaussians of identical width and scattering amplitude, $A_1 = A_2 = 3$ Å and $b_1 = b_2 = 1$, respectively (note that scattering amplitude has units of length [Schoenborn, 1975]). A representative value of $R_s = 0.03$ is also plotted; for neutron and x-ray diffraction studies of L_α DOPC, R_s equals 0.033 and 0.025, respectively.

Fig. 5 illustrates several points. First, with the exception of ~ 3 Å at either edge of the bilayer leaflet, R is relatively invariant with respect to Z_1. The jagged appearance of the plots of R is a consequence of the use of absolute values of structure factors in the definition of R (Eq. 4). The absolute value makes the cosine terms of (Eq. 2) positive-definite and gives rise to the jagged lines. Also, there are values of Z_1 and ΔZ which result in $R = 0$, i.e., when $h/d = n/(2Z_1 + \Delta Z)$ and $h/d = (1/2)([2n + 1] / [2 Z_1 + \Delta Z])$ for even and odd nonnegative integer n, respectively. For instance, $Z_1 = 12$ Å and $\Delta Z = 1$ Å leads to a zero value of R so the data cannot discriminate two Gaussians. Fortunately, these "undeterminable" points are sparse. Second, the value of this constant region of R is roughly proportional to ΔZ; i.e. $R(\Delta Z = 0.3) \approx 3R(\Delta Z = 0.1)$. Third, and most important for this discussion, differences in position of 0.15 Å or more are discernible above experimental noise. Thus, given two model distributions differing by 0.15 Å or more in their centers, one of them will provide a better fit to the data and, crucially, the better quality of the fit is statistically significant.

The resolution of structural features will also depend upon their widths and amplitudes. The width of a distribution influences the number of diffraction orders observed (Fig. 3), so the contribution of a structural feature to the observed diffraction, especially at higher orders, decreases as its width increases. This reduced contribution weights the resolution of the model, decreasing the accuracy with which the wider distribution can be determined and increasing the accuracy with which the narrower distribution can be determined. In Fig. 6 *A* a Gaussian of width $A_1 = 6$ Å is centered at Z_1 and another Gaussian of width $A_2 = 3$ Å at $Z_1 + \Delta Z$. Compared to two Gaussians of identical 3 Å width (Fig. 5), the model is more sensitive to variation in the position of the narrower (3 Å) Gaussian; a peak separa-

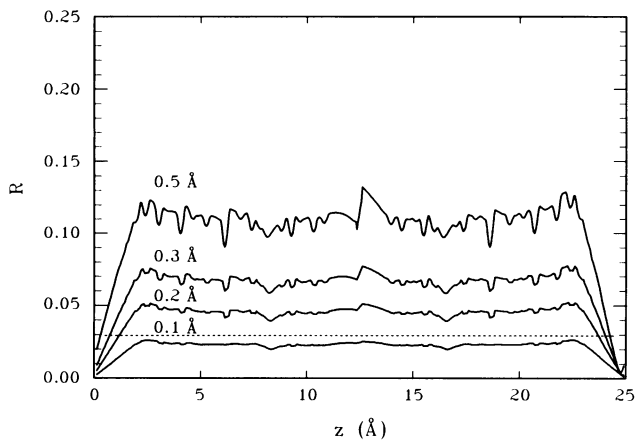

FIGURE 5 R factor as a function of bilayer position Z_1 and increment ΔZ. $A_1 = A_2 = 3$ Å; $b_1 = b_2 = 1$. R is defined in Eq. 4. From top to bottom, the curves represent increments $\Delta Z = 0.5$, 0.3, 0.2, 0.1 Å, respectively. With the exception of ≈3 Å at either edge of the $[0, d/2]$ interval, R is roughly constant and scales with ΔZ. The dashed line denotes $R_s = 0.03$. Shifts of 0.15 Å or more in the position of Gaussian 2 are distinguishable above the experimental uncertainty R_s.

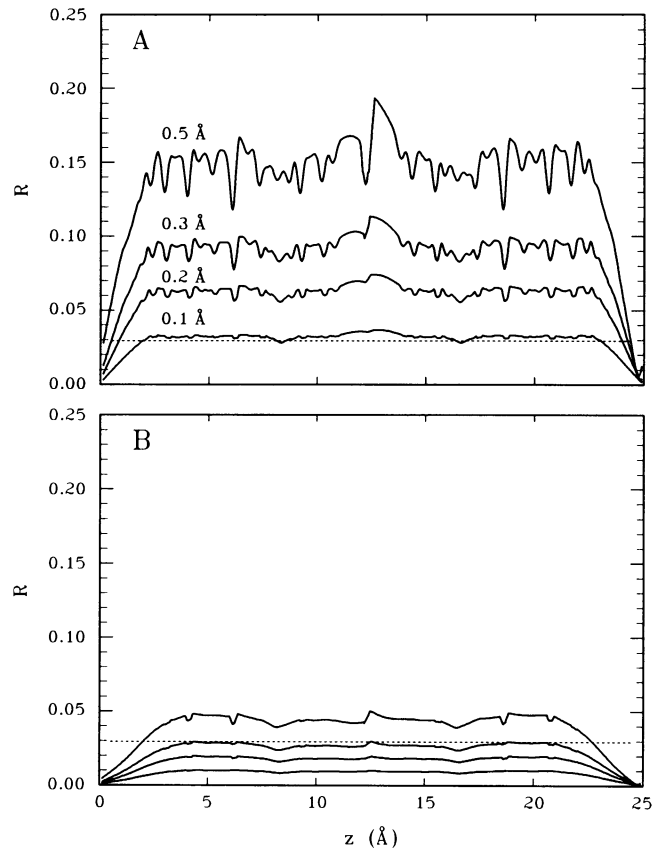

FIGURE 6 R factor as a function of bilayer position Z_1 and increment ΔZ. With the exception of ≈3 Å at either edge of the $[0, d/2]$ interval, R is roughly constant and scales with ΔZ. The dashed line denotes $R_s = 0.03$. (*A*) $A_1 = 6$ Å; $A_2 = 3$ Å; $b_1 = b_2 = 1$. Shifts of 0.1 Å or more in position of Gaussian 2 are distinguishable above the experimental uncertainty R_s. (*B*) $A_1 = 3$ Å; $A_2 = 6$ Å; $b_1 = b_2 = 1$. Shifts of 0.35 Å or more in position of Gaussian 2 are distinguishable above the experimental uncertainty R_s.

tion of 0.1 Å is experimentally discernible as opposed to 0.15 Å in Fig. 5. Conversely, the model is less sensitive to a shift in the wider Gaussian (Fig. 6 *B*); a separation of 0.35 Å or more is now the limit of resolution. Similar behavior is observed for two Gaussians of identical width (3 Å) but differing in scattering amplitude by a factor of five; the resolution of the larger amplitude peak is enhanced whereas the resolution of the smaller amplitude peak is reduced (data not shown).

In neutron diffraction, structural features can differ in sign as well as magnitude of scattering length (Schoenborn, 1975). In Fig. 7 *A*, a Gaussian of width $A_1 = 3$ Å and amplitude $b_1 = 2$ is centered at Z_1 and another Gaussian of width $A_2 = 3$ Å and amplitude $b_2 = -1$ at $Z_1 + \Delta Z$. The difference in sign, as well as magnitude, increases the resolution of the model; a peak separation of 0.05 Å or more is above experimental noise. The model is equally sensitive to shifts in the positive amplitude peak position $Z_1 + \Delta Z$ relative to fixing the negative peak at Z_1 (data not shown). Fig. 7 *B* illustrates how increased width of a structural feature can effectively cancel out the enhanced sensitivity due to increased peak amplitude. Changing A_2 from 3 to 6 Å increases the resolvable peak separation from 0.05 to 0.4 Å.

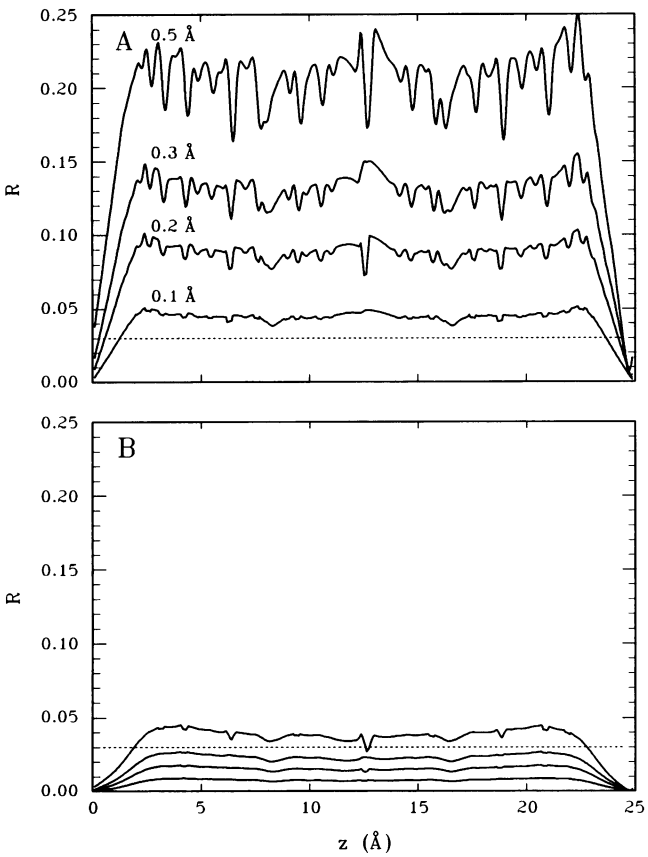

FIGURE 7 *R* factor as a function of bilayer position Z_1 and increment ΔZ. With the exception of ≈3 Å at either edge of the $[0, d/2]$ interval, *R* is roughly constant and scales with ΔZ. The dashed line denotes R_s = 0.03. (*A*) $A_1 = A_2 = 3$ Å; $b_1 = 2$; $b_2 = -1$. Shifts of 0.05 Å or more in position of Gaussian 2 are distinguishable above the experimental uncertainty R_s. (*B*) $A_1 = 3$ Å; $A_2 = 6$ Å; $b_1 = 2$; $b_2 = -1$. Shifts of 0.4 Å or more in position of Gaussian 2 are distinguishable above the experimental uncertainty R_s.

The one- and two-Gaussian models used in these calculations are certainly much simpler than the actual quasimolecular models used in the determination of fluid bilayer structure. As we will discuss in the second paper of the series, a typical fluid bilayer can be represented by 5–10 Gaussian distributions. However, the calculations in this section clearly illustrate two major aspects of structural resolution that are valid for more complicated quasimolecular models. First, the width $2 \cdot A$ of a scattering region is given approximately by d/h_{max}. The 1/e half-width of a Gaussian distribution determines the number h_{max} of observable structure factors as shown by Eq. 3. In a model calculation (Fig. 3), a single Gaussian of 1/e half-width $A = 3$ Å in a bilayer of repeat $d = 50$ Å yields nine orders of observable diffraction whereas a narrower ($A = 1$ Å) Gaussian yields 29 orders. These results indicate that the characteristic length scale of the bilayer is $\sim d/h_{max}$. Second, based upon typical experimental errors, the positions of scattering regions within the bilayer can be determined with a precision of 0.1–0.5 Å. The resolution of separate scattering regions within the bilayer depends upon their relative scattering lengths as well as their widths and peak separations. As its scattering length increases, a region is more readily located within the bilayer. Increasing its width, which reduces the number and amplitude of structure factors (Eq. 2), makes it harder to resolve from other scattering centers. The calculation of Eq. 4 for a number of two-Gaussian models, shown in Figs. 5–7, is the basis of our estimate of precision.

DISCUSSION

The importance of Gaussian models in the interpretation of diffraction data is clear: they permit precise determination of the centers and widths of significant scattering features of lipid molecules in fluid bilayers (King and White, 1986; Jacobs and White, 1989; Wiener et al., 1989). Rand and Luzzati (1968) noted that the discrimination of such models is "quite severe." Our analysis demonstrates quantitatively the sensitivity of calculated structure factors $F(h)$ to model parameters. In the second (Wiener and White, 1990) and subsequent papers of this series, the quasimolecular model of King and White (1986) will be thoroughly explored and used

for the joint analysis of neutron and x-ray diffraction data of liquid-crystalline L_α DOPC bilayers. The resulting profiles, which represent the scattering centers as Gaussian functions, provide a physically meaningful representation of the distribution of matter across the bilayer. The peak position of each Gaussian provides a precise determination of the center-of-scattering of the constituents of that quasi-molecular component and the width of the distribution can be used to estimate the range of accessible motion of the moiety. Many models of the bilayer "work" in reciprocal space by fitting the data; the quasimolecular model is notable for the information content of its real-space profile.

The number of observable diffraction orders contains information about the fundamental structure of the bilayer and, as we shall show in the next paper (Wiener and White, 1990), provides information on the number of Gaussians required to model it. The canonical resolution, d/h_{max}, is the most appropriate length scale with which to describe the bilayer, i.e., it is the characteristic size of the molecular subunit that is discernible in the long-time (and space) average of a diffraction experiment. If an experiment records 10 diffraction orders from a bilayer with a d-spacing of 50 Å, the principal scattering centers are $\sim$5 Å wide. In the context of the quasimolecular model, regions of the molecule that make the largest contributions to the total scattering are described by Gaussian distributions of 1/e half-widths of $\sim$2.5 Å. Other regions of the molecule that contribute less to the total scattering may be more widely dispersed with larger widths, but the lower bound on distribution width is given approximately by the canonical resolution d/h_{max}. Because of the importance of the canonical resolution in the determination of the appropriate length-scale, it is critical that all of the observable diffraction orders be measured. To determine the limits of spatial resolution, it is important to have a reasonable estimate of the experimental errors of the structure factors. A model based upon an imperfect data set, i.e., one that excludes significant higher order structure factors, is likely to result in an incorrect model of the bilayer. The Fourier profile resulting from imperfect data will have Fourier ripples (Fig. 4) that confound the analysis.

Through a series of simple model calculations, we have demonstrated that analysis of membrane diffraction data can yield precise determinations of the centers of scattering density in liquid-crystalline bilayers. The physical basis underlying these calculations is the observation that multilamellar liquid-crystalline arrays, particularly single component phospholipids and simple mixtures, are described by the convolution of a nearly perfect lattice with a highly disordered unit cell. The model calculations presented here, while not an exhaustive survey of quasimolecular models, indicate the variety of behavior expected in the analysis of diffraction data with more complicated quasimolecular models. In subsequent papers, a thorough error analysis procedure will be utilized, rather than the simple model calculations shown here, to determine the uncertainties in model parameters. Going beyond the two-body models presented here to more realistic models with a greater number of Gaussians complicates the details of determining the uncertainties of model parameters, but the basic relations are expected to remain the same. As the width of a structural feature increases, the precision with which its center can be determined will decrease. The larger the scattering amplitude of a model component, the more precisely it will be located within the bilayer. This latter observation is completely consistent with the precise assignment of the major positive peaks in x-ray and neutron density profiles to phosphate and carbonyl moieties, respectively (Janiak et al., 1979; Franks and Lieb, 1979; McIntosh and Simon, 1986; King and White, 1986).

We are pleased to acknowledge the technical advice of Drs. Benno Schoenborn and Anand Saxena at Brookhaven National Laboratory. We are particularly indebted to Dr. Dieter Schneider for his help with the analysis of the neutron data. Dr. Robert V. McDaniel and Mr. Harold J. Levy modified the densitometer for use in scanning x-ray films.

This work was supported by grants from the National Science Foundation (DMB-880743) and the National Institute of General Medical Sciences (GM-37291). Parts of the research were carried out using the High Flux Beam Reactor at Brookhaven National Laboratory, Upton, Long Island, NY, under the auspices of the U.S. Department of Energy with the additional support of the National Science Foundation.

Received for publication 27 July 1990 and in final form 24 September 1990.

REFERENCES

Bacon, G. E. 1975. Neutron Diffraction. 3rd ed. Clarendon Press, Oxford. 636 pp.

Blasie, J. K., B. P. Schoenborn, and G. Zaccai. 1975. Direct methods for the analysis of lamellar neutron diffraction from oriented multilayers: a difference Patterson deconvolution approach. *Brookhaven Symp. Biol.* 27:III58–III67.

Blaurock, A. E. 1982. Evidence of bilayer structure and of membrane interactions from x-ray diffraction analysis. *Biochim. Biophys. Acta.* 650:167–207.

Bragg, W. L., and J. West. 1930. A note on the representation of crystal structure by Fourier series. *Philosophical Magazine and Journal of Science.* 10:823–841.

Bretscher, M. S., and M. C. Raff. 1975. Mammalian plasma membranes. *Nature (Lond.).* 258:43–49.

Büldt, G., H. U. Gally, J. Seelig, and G. Zaccai. 1979. Neutron diffraction studies on phosphatidylcholine model membranes. I. Head group conformation. *J. Mol. Biol.* 134:673–691.

Dorset, D. L., A. K. Massalski, and J. R. Fryer. 1987. Interpretation of lamellar electron diffraction data from phospholipids. *Z. Naturforsch.* A42:381–391.

Elliott, A. 1965. The use of toroidal reflecting surfaces in x-ray diffraction cameras. *J. Sci. Instrum.* 42:312–316.

Franks, N. P. 1976. Structural analysis of hydrated egg lecithin and cholesterol bilayers. I. X-ray diffraction. *J. Mol. Biol.* 100:345–358.

Franks, N. P., and Y. K. Levine. 1981. Low-angle x-ray diffraction. *In* Membrane Spectroscopy. E. Grell, editor. Springer-Verlag, Berlin. 437–487.

Franks, N. P., and W. R. Lieb. 1979. The structure of lipid bilayers and the effects of general anaesthetics: an x-ray and neutron diffraction study. *J. Mol. Biol.* 133:469–500.

Franks, N. P., V. Melchior, D. A. Kirschner, and D. L. D. Caspar. 1982. Structure of myelin lipid bilayers. Changes during maturation. *J. Mol. Biol.* 155:133–153.

Glusker, J. P. (ed) 1981. Structural Crystallography in Chemistry and Biology. Hutchinson Ross Publishing Co., Stroudsburg, PA. 421 pp.

Hauser, H., I. Pascher, R. H. Pearson, and S. Sundell. 1981. Preferred conformation and molecular packing of phosphatidylethanolamine and phosphatidylcholine. *Biochim. Biophys. Acta.* 650:21–51.

Hitchcock, P. B., R. Mason, and G. G. Shipley. 1975. Phospholipid arrangements in multilayers and artificial membranes: quantitative analysis of the x-ray diffraction data from a multilayer of 1,2-dimyristoyl-DL-phosphatidylethanolamine. *J. Mol. Biol.* 94:297–299.

Hosemann, R., and S. N. Bagchi. 1962. Direct Analysis of Diffraction by Matter. North-Holland Publishing Co., Amsterdam. 734 pp.

Inoko, Y., and T. Mitsui. 1978. Structural parameters of dipalmitoyl phosphatidylcholine lamellar phases and bilayer phase transitions. *J. Phys. Soc. Japan.* 44:1918–1924.

Jacobs, R. E., and S. H. White. 1989. The nature of the hydrophobic binding of small peptides at the bilayer interface: Implications for the insertion of transbilayer helices. *Biochemistry.* 28:3421–3437.

Janiak, M. J., D. M. Small, and G. G. Shipley. 1979. Temperature and compositional dependence of the structure of hydrated dimyristoyl lecithin. *J. Biol. Chem.* 254:6068–6078.

King, G. I., and S. H. White. 1986. Determining bilayer hydrocarbon thickness from neutron diffraction measurements using strip-function models. *Biophys. J.* 49:1047–1054.

Kuriyan, J., G. A. Petsko, R. M. Levy, and M. Karplus. 1986. Effect of anisotropy and anharmonicity on protein crystallographic refinement. An evaluation by molecular dynamics. *J. Mol. Biol.* 190:227–254.

Levine, Y. K., and M. H. F. Wilkins. 1971. Structure of oriented lipid bilayers. *Nat. New Biol.* 230:69–72.

McIntosh, T. J., and S. A. Simon. 1986. Hydration force and bilayer deformation: A reevaluation. *Biochemistry.* 25:4058–4066.

McIntosh, T. J., R. V. McDaniel, and S. A. Simon. 1983. Induction of an interdigitated gel phase in fully hydrated phosphatidylcholine bilayers. *Biochim. Biophys. Acta.* 731:109–114.

Mitsui, T. 1978. X-ray diffraction studies of membranes. *Adv. Biophys.* 10:97–135.

Perutz, M. F. 1942. X-ray analysis of haemoglobin. *Nature (Lond.).* 149:491–494.

Phillips, W. C., and G. N. Phillips. 1985. Two new x-ray films: conditions for optimum development and calibration of response. *J. Appl. Cryst.* 18:3–7.

Ranck, J. L., T. Keira, and V. Luzzati. 1977. A novel packing of the hydrocarbon chains in lipids: the low temperature phases of dipalmitoyl phosphatidyl-glycerol. *Biochim. Biophys. Acta.* 488:432–441.

Rand, R. P., and V. Luzzati. 1968. X-ray diffraction study in water of lipids extracted from human erythrocytes: the position of cholesterol in the lipid lamellae. *Biophys. J.* 8:125–137.

Ringe, D., and G. A. Petsko. 1986. Study of protein dynamics by x-ray diffraction. *Methods Enzymol.* 131:389–433.

Sakurai, I., S. Iwayanagi, T. Sakurai, and T. Seto. 1977. X-ray study of egg-yolk lecithin: Unit cell data and electron density profile. *J. Mol. Biol.* 117:285–291.

Schoenborn, B. P. 1975. Advantages of neutron scattering for biological structure analysis. *Brookhaven Symp. Biol.* 27:I10–I17.

Schoenborn, B. P. 1983. Peak-shape analysis for protein neutron crystallography with position-sensitive detectors. *Acta Cryst.* A39:315–321.

Schwartz, S., J. E. Cain, E. A. Dratz, and J. K. Blasie. 1975. An analysis of lamellar x-ray diffraction from disordered membrane multilayers with application to data from retinal rod outer segments. *Biophys. J.* 15:1201–1233.

Sirota, E. B., G. S. Smith, C. R. Safinya, R. J. Plano, and N. A. Clark. 1988. X-ray scattering studies of aligned, stacked surfactant membranes. *Science (Wash. DC).* 242:1406–1409.

Smith, G. S., C. R. Safinya, D. Roux, and N. A. Clark. 1987. X-ray study of freely suspended films of a multilamellar lipid system. *Mol. Cryst. Liq. Cryst.* 144:235–255.

Smith, G. S., E. B. Sirota, C. R. Sifinya, and N. A. Clark. 1988. Structure of the L_{β}' phases in a hydrated phosphatidylcholine multimembrane. *Phys. Rev. Lett.* 60:813–816.

Suwalsky, M., and L. Duk. 1987. Structure determination of oriented films of L-α-dimyristoylphosphatidylethanolamine (DMPE). *Makromol. Chem.* 188:599–606.

Warren, B. E. 1969. X-ray Diffraction. Addison-Wesley, Reading, MA. 381 pp.

White, S. H., G. I. King, and J. E. Cain. 1981. Location of hexane in lipid bilayers determined by neutron diffraction. *Nature (Lond.).* 290:161–163.

Wiener, M. C., and S. H. White. 1990. Fluid bilayer structure determination by the combined use of x-ray and neutron diffraction. II. The "composition space" refinement method. *Biophys. J.* 59:174–185.

Wiener, M. C., R. M. Suter, and J. F. Nagle. 1989. Structure of the fully hydrated gel phase of dipalmitoylphosphatidylcholine. *Biophys. J.* 55:315–325.

Willis, B. T. M., and A. W. Pryor. 1975. Thermal Vibrations in Crystallography. Cambridge University Press, Cambridge, UK. 280 pp.

Worcester, D. L. 1975. Neutron diffraction studies of biological membranes and membrane components. *Brookhaven Symp. Biol.* 27:III37–III57.

Worcester, D. L., and N. P. Franks. 1976. Structural analysis of hydrated egg lecithin and cholesterol bilayers II. Neutron diffraction. *J. Mol. Biol.* 100:359–378.

Worthington, C. R. 1969. The interpretation of low-angle x-ray data from planar and concentric multilayered structures: the use of one-dimensional electron density strip models. *Biophys. J.* 9:222–234.

Zaccai, G., G. Büldt, A. Seelig, and J. Seelig. 1979. Neutron diffraction studies on phosphatidylcholine model membranes II. Chain conformation and segmental disorder. *J. Mol. Biol.* 134:693–706.